Available online at www.sciencedirect.com
ScienceDirect
Bioorganic & Medicinal Chemistry 15 (2007) 7795–7802
Bioorganic & Medicinal Chemistry

Virtual screening and bioassay study of novel inhibitors for dengue virus mRNA cap (nucleoside-2′*O*)-methyltransferase

Victor B. Luzhkov,[a] Barbara Selisko,[b] Anneli Nordqvist,[c] Frédéric Peyrane,[b] Etienne Decroly,[b] Karine Alvarez,[b] Anders Karlen,[c] Bruno Canard[b] and Johan Åqvist[a,*]

[a]*Department of Cell and Molecular Biology, Uppsala University, BMC, Box 596, S-751 24 Uppsala, Sweden*
[b]*Centre National de la Recherche Scientifique and Universités d'Aix-Marseille I et II, UMR 6098, Architecture et Fonction des Macromolécules Biologiques, AFMB-CNRS-ESIL, Case 925, 163 Avenue de Luminy, 13288 Marseille Cedex 9, France*
[c]*Department of Medicinal Chemistry, Uppsala University, BMC, Box 574, S-751 23 Uppsala, Sweden*

Received 15 March 2007; revised 17 August 2007; accepted 24 August 2007
Available online 29 August 2007

Abstract—We report high-throughput structure-based virtual screening of putative *Flavivirus* 2′-*O*-methyltransferase inhibitors together with results from subsequent bioassay tests of selected compounds. Potential inhibitors for the *S*-adenosylmethionine binding site were explored using 2D similarity searching, pharmacophore filtering and docking. The inhibitory activities of 15 top-ranking compounds from the docking calculations were tested on a recombinant methyltransferase with the RNA substrate ^{7Me}GpppAC$_5$. Local and global docking simulations were combined to estimate the ligand selectivity for the target site. The results of the combined computational and experimental screening identified a novel inhibitor, with a previously unknown scaffold, that has an IC_{50} value of 60 μM.

1. Introduction

Development of effective pharmaceuticals acting on species from the genus *Flavivirus* – the underlying cause of several serious diseases in humans (e.g., encephalitis and haemorrhagic symptoms) – presents an important and complex problem for medicinal chemistry.[1] New promising antiviral agents may be found among inhibitors of the enzymes involved in viral replication. Possible targets for inhibitor search include the viral mRNA cap methyltransferases (MTases), which are involved in the posttranscriptional modification (capping) of viral RNAs and, in particular, catalyze methylation of the N7-position of the cap guanine (guanine-N7 MTase or N7MTase) and/or of the ribose 2′*O*-position of the first transcribed nucleotide (nucleoside-2′-*O* MTase or 2′OMTase).[2–4] A number of chemical and functional studies have previously addressed DNA and RNA methyltransferases from various sources as potential inhibitor targets.[5–14]

The crystal structure of the MTase domain of the dengue virus non-structural protein NS5 (NS5MTase$_{DV}$) in complexes with the co-product of the methyl transfer, *S*-adenosyl-L-homocysteine (AdoHcy) and GTP-analogues discloses important features related to the protein function.[15,16] NS5MTase$_{DV}$ has an overall globular shape with a central subdomain adopting a typical fold of AdoMet-dependent MTases with a seven-stranded central β-sheet surrounded by six helices.[15,17,18] It differs from the consensus topology by the absence of the B and C α-helices between the β strands 2 and 3, and 3 and 4, respectively.[15] Structure determination of two complexes defined two binding sites, one for the methylating cofactor *S*-adenosylmethionine (AdoMet) and AdoHcy, and a second site for GTP-analogues situated on an N-terminal subdomain.[15,16] The AdoMet-binding position is preserved and similar in all AdoMet-dependent MTases. Because of the appropriate distance to the AdoMet-binding site, the GTP binding site was proposed to harbor the cap guanine during 2′*O*-methylation.[15] This activity has been demonstrated using small

Keywords: Flavivirus methyltransferase inhibitor; Drug design; Virtual screening; Docking.
* Corresponding author. Tel.: +46 18 4714109; fax: +46 18 536971; e-mail: aqvist@xray.bmc.uu.se

0968-0896/$ - see front matter © 2007 Elsevier Ltd. All rights reserved.
doi:10.1016/j.bmc.2007.08.049

capped RNA substrates $^{7Me\pm}GpppAC_n$.[15,19] The positively charged zone between both sites indicates the RNA-binding region, which continues beyond the active site. A recent publication demonstrated that NS5MTase$_{DV}$ bears not only the 2′OMTase but also the N7MTase activity of dengue virus and that N7-methylation precedes 2′*O*-methylation.[20] The same group had previously shown that this also applies to the cognate NS5MTase domain of the flavivirus West Nile virus (WNV) and that the C-terminal RNA-dependent RNA polymerase (RdRp) domain of NS5 does not influence the enzymatic activities of the MTase domain.[21] Finally, it was demonstrated that the N7MTase activity was absolutely essential for WNV growth in cell culture.[20] Thus, the NS5MTase domain is of utmost interest to be explored as a target for the discovery and development of anti-*Flavivirus* drugs and there especially the AdoMet-binding site, which is involved in both MTase activities. In this context it is of interest to note that the residues, which form the AdoMet-binding site of AdoMet-dependent MTases, are poorly conserved,[18] which will be very important for the specificity of a *Flavivirus* MTase inhibitor.

Structure-based computational approaches for evaluating binding propensities within large ligand sets are widely used in modern rational drug design (e.g., Refs. 22–27 and references therein). An important class of such methods is based on virtual screening with a pharmacophore or a 2D pattern derived from known active substances, as the search query. A second class of virtual screening methods is provided by docking and scoring techniques that predict the positions of bound ligands and the related binding affinities for cases where the 3D atomic structure of the protein target is known. Advanced docking algorithms can in general accurately sample the conformational space of protein–ligand complexes, including those of conformationally flexible binders. Analytical scoring functions of differing composition and accuracy are used for estimating protein–solvent–ligand interaction energies and to rank the binding affinities of the docked solutions. Both high-throughput virtual library screens and docking methods may generate false hits and miss promising compounds,[23] but despite the inherent limitations the virtual screening methods provide a valuable tool for rational selection of potential hits for bioassay studies.

The aim of the present work is to identify new classes of flavivirus NS5MTase$_{Dv}$ inhibitors using structure-based computational approaches and subsequent bioassays. The convoluted surface of the protein, which is able to host multiple ligands, opens diverse possibilities for drug design. Indeed, inhibitory activity against different MTases was found earlier for a number of AdoMet/AdoHcy analogues,[9–11] DNA with modified nucleosides,[13] and organoselenium compounds.[14] The study of the adenosine derivatives 3-deazaadenosine and neplanocin, which interfere with influenza virus replication, indicated that these compounds act on presumably different methyltransferases.[9] The natural AdoMet analogue sinefungin also demonstrated inhibition of the yeast and fungal mRNA cap methyltransferases.[11] On the other hand, the antiviral nucleoside analogue drug ribavirin, the triphosphate derivative of which binds directly to NS5MTase$_{Dv}$,[16] shows only weak activity against flaviviruses.[1] Inhibition of NS5MTase$_{Dv}$ by ribavirin 5′-triphosphate is also weak.[16] The three-dimensional structure of the tertiary complex of ribavirin 5′-triphosphate (at the GTP-binding site), AdoHcy, and NS5MTase$_{Dv}$ shows that the nucleoside and AdoHcy-binding sites are essentially separated in space.[16] In the present study, we focus on molecules which are complementary to the AdoMet/AdoHcy-binding cavity of NS5MTase$_{Dv}$.

The quest for novel binders involved three steps: database similarity/pharmacophore search → docking of the filtered sets → measurements of inhibition, where the set of possible molecules was sequentially reduced down to an amount acceptable for bioassay testing of their effect on the 2′OMTase activity of the recombinant NS5MTase$_{Dv}$ domain in vitro. A similar combination of pharmacophore screens and docking proved successful, for example, in a recent study of *Plasmodium falciparum* DHFR inhibitors.[24] The whole search procedure was repeated twice, in which case the database screening in the second round was performed using structural motives from the hit obtained in the first round. In the end this approach yielded several diverse classes of potentially good binders and allowed us to identify a new active compound with a scaffold unrelated to the known MTase inhibitors.

2. Results and discussion

2.1. Database search for structurally compliant binders

We started the search for NS5MTase$_{Dv}$ inhibitors by performing a pharmacophore and a 2D similarity search of a database of 2.1 million commercially available compounds. The search queries were generated using information from the AdoHcy structure in complex with the protein. The corresponding pharmacophore model consists of four hydrogen bond acceptors, two hydrogen bond donors, and two hydrophobic centers with a tolerance criterion of 2 Å (Fig. 1a). A flexible pharmacophore search was set up so as to find at least one feature in each end of the molecule (see Fig. 1a) and 895 hits were identified matching the described pattern. In the query for the 2D similarity search, all hydrogens of AdoHcy were removed, the sugar moiety was simplified and the adenine group was replaced with a phenyl moiety (Fig. 1a). The search procedure was set up to identify compounds having a similarity index larger than 40, as calculated by the Tanimoto method, and a molecular weight higher than 250 g/mol. The latter search resulted in 1671 hits. Preliminary searches with the adenine moiety intact only returned chemically protected adenosinetriphosphate analogues. The three-dimensional structures of the compounds extracted from the pharmacophore and similarity searches were subject to geometry optimization. Subsequent ligand preparation, including generation of tautomers, stereoisomers, ring conformations, and different ionization states, resulted in a total of 7836 structures.

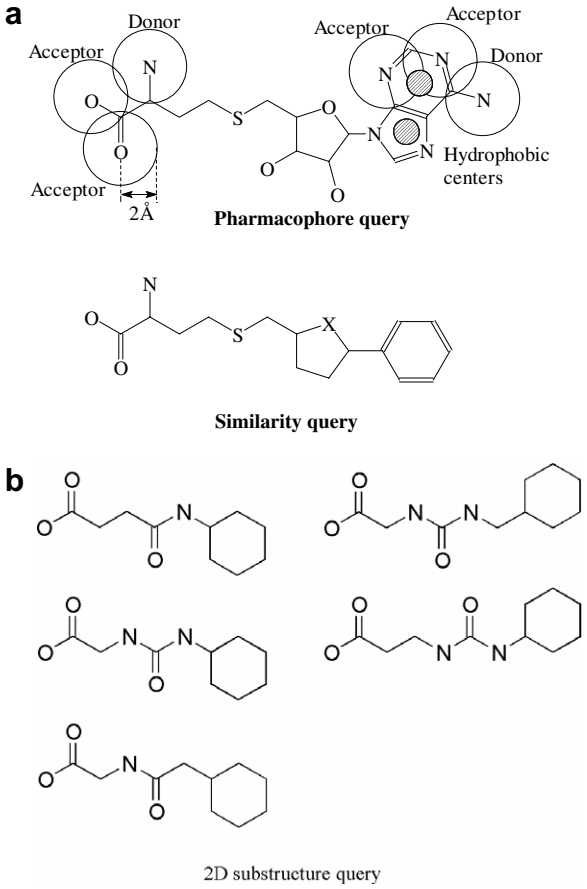

Figure 1. The query derived from AdoHcy used in the first round of database searching (a), and that derived from **7** used in the second round (b). X denotes any atom.

To follow up on the identified inhibitor (vide infra) a second round of database screening was performed, where a 2D substructure search was carried out based on several scaffolds derived from the structure of the hit identified in the first round (**7** in Fig. 2a). The corresponding topologies typically included a six-membered ring (a simplified tricyclic system), an amide or urea linker, and a carboxyl group (Fig. 1b). The limit for the molecular weight was set as in the first round. Overall, the second round of database searching and the following ligand preparation produced 3225 structures.

2.2. Docking of the filtered ligand set

The ligand sets from the database searches were docked and ranked according to the docking scores. The AdoMet-binding cleft of NS5MTase$_{Dv}$ was selected as the prime target area in the first docking round. We started by evaluating the performance of the scoring functions (GoldScore[28,29] and ChemScore[30]) included in the GOLD[28,29] program for the well-described case of AdoHcy binding.[15] The docking region was confined to a 13 Å radius sphere around the backbone oxygen of Gly81 located near the center of the binding site. We will refer to this as local docking in contrast to global docking described below. Four crystallographic waters were added to the active site space (HOH 5, 35, 50, 51 in the NS5MTase$_{DV}$ structure with the PDB code 1L9K). These solvent molecules are close to the bound AdoHcy in 1L9K and hence can contribute to ligand stabilization. GOLD allows to explore active configurations of explicit waters by switching the water interactions ON and OFF and varying water orientations during the docking scans. The AdoHcy structures docked using the GoldScore function accurately reproduce its experimental position. The root mean square difference between the experimental and the three top-score structures is only 1.0–1.1 Å. The occupancy of the solvent molecule HOH5 is ON, HOH50 is either ON or OFF, whereas HOH35 and HOH51 are OFF in the predicted protein–ligand complexes. Such occupancies are in a reasonable agreement with the qualitative picture of the ligand interactions in the binding site (see Fig. 1 of the Supplementary material). In particular, HOH5 and HOH50 are buried at the protein–ligand interface close to the amino acid tail of AdoHcy, while the positions of HOH35 and HOH51 are solvent exposed. The ChemScore based docking, unlike the GoldScore case, severely misplaces AdoHcy, reversing its orientation in the binding site and putting the docked adenine moiety in the binding pocket for the amino acid tail. We have also checked the docked solutions for the NS5MTase$_{Dv}$–AdoMet complex where the experimental structure is not known. Docking of AdoMet with the GoldScore and ChemScore functions produced similar structures to the AdoHcy case, that is, ChemScore again appears to misplace the ligand compared to the most relevant experimental structure.

Docking of 7836 compounds generated from the first round of database searching was carried out using the GoldScore function with the same active site space as in the AdoHcy test case. The entire data set was split, using hierarchial clustering on atom pairs and fingerprints, into 20 structurally diverse ligand clusters which were docked separately using the program settings for faster optimization. The top-ranking 5–20 hits from each cluster (depending on its size) were then merged into a set of 230 ligands which was redocked using the program settings for accurate search. The 30 highest scoring structures were further considered for final compound selection. However, only 19 unique compounds were found in the list of top 30 solutions, since the same chemical structure in some cases is present from different vendors and as different isomers from the ligand preparation step. By using this straightforward ligand ranking we implicitly assume that the computed docking scores may at least partially reflect experimental binding affinities. The derived data set includes compounds from several clusters with fairly diverse chemical scaffolds. However, in most cases the docked structures sufficiently closely match the template position of AdoHcy.

In an attempt to increase the amount of useful information, we have also performed global docking of the 230 best scoring compounds, which were earlier determined from the local docking procedure. The global docking was set up in such a way as to consider a broader area of the protein surface, which could reveal multiple binding sites as well as indicating the selectivity of a given

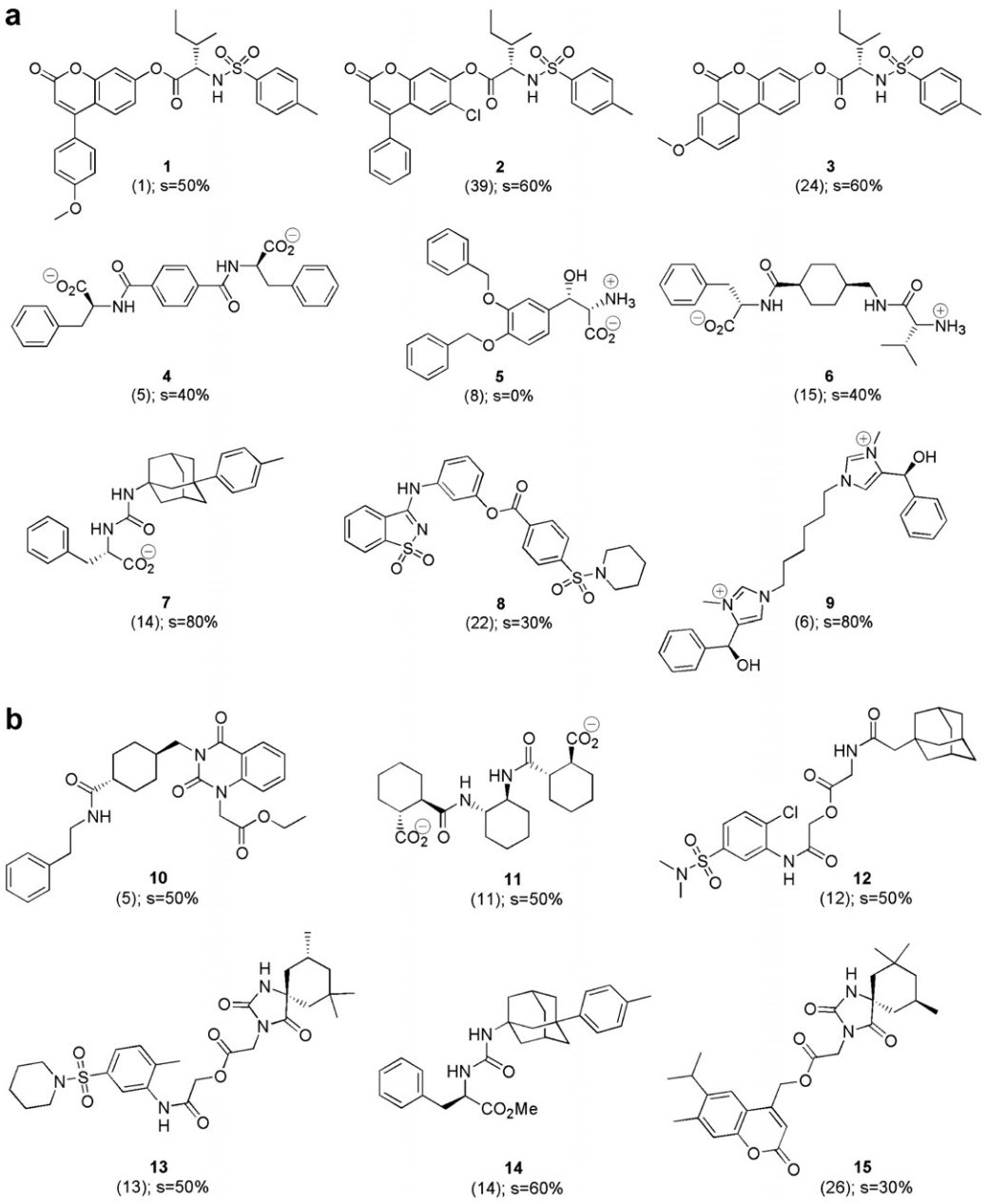

Figure 2. The selected top-scoring chemical structures from the first (a) and second (b) rounds of docking simulations. For each structure, the numbers in parentheses show the ranks from the local docking. The 's' index denotes the percentage of solutions docked at the target site in the global docking simulations. The initial docking procedure included all possible stereoisomers of the ligands. The stereochemistry of the top-ranked docked stereoisomer is indicated in the figure, but only four of the tested ligands are synthesized from enantiomerically pure amino acids and the rest of the compounds are non-chiral or tested as racemic mixtures (see Section 4.3). For compound **2**, the D-form had the highest score (No. 7) and the L-form scored almost as good (No. 39); however, only the commercially available L-form could be included in the final selection and evaluated in the biological assay. Note also in this respect that the D-form of ligand **1** ranked second in the local docking. Compound **6** was docked as both *cis* and *trans*-isomer, where the *cis*-isomer had the highest score.

ligand for the primary target site. The region for global docking was delineated by a 22 Å radius sphere centered at the NZ atom of Lys181, which fully covers the AdoMet- and GTP-binding sites as well as the connecting deep cavity. The distribution of the top-ranking docked positions at the protein cavity shows that approximately only half of the considered ligand set can be considered selective for the AdoMet-binding cleft. Figure 3 vividly demonstrates the corresponding shift of spatial distribution of the docked ligands from the local and global docking simulations.

After the first round of docking simulations, 9 compounds, that is, **1**–**9**, were selected for testing their inhibitory activity, Figure 2a. The selection included at least one compound from each structural cluster of the predicted top 30 binders. The binding ranks of molecules **1**–**9** from the local docking simulations are provided in Figure 2a. The selectivity indices, also displayed in Figure 2a, indicate the percent of docked positions (out of 10 generated solutions) which belong to the AdoMet cavity for each ligand. Many of the 230 compounds are actually larger than AdoHcy and, hence, are par-

tially positioned outside the AdoHcy cavity. Therefore, when inspecting docked solutions we used only qualitative criteria for selectivity. That is, a ligand was considered as belonging to the target site if the docked pose distinctly overlaps with the ribose and adenine moieties of the bound AdoHcy. We applied such loose criteria for selectivity because in many cases the ligands, which upon docking find a position at the target site, have low overlap with the amino acid tail of the bound AdoHcy. It was also noticed that many compounds with common chemical structures show significantly varying docked poses and selectivity toward the target site. The highest selectivity scores in the global docking test are predicted for the adamantyl urea derivative **7** and imidazole derivative **9**.

The measurements of inhibitory activity (vide infra) showed that the majority of the predicted binders from the first round can only be viewed as weak inhibitors of NS5MTase$_{Dv}$. Compound **7** showed the highest activity among the tested compounds. The database similarity search, using scaffolds of **7** (vide supra, Fig. 1b) extracted 3225 structures. The latter data set was docked to the previously described 13 Å and 22 Å spheres around the protein target site (local and global docking, respectively). Prior to docking the entire data set was split into five structurally diverse clusters, and each of them was docked separately. Subsequently, the best 5–20 ligands from each cluster were merged into the set of 65 compounds and redocked together using the program settings for stringent docking. Analysis of the new predicted top-docked solutions showed that some of them had already been found in the first round of the virtual screening calculations. In particular, this refers to ligand **7**, which received several high scores in the second round of docking. The new structures, which were additionally selected for bioassay measurements among the list of top 30 binders in the second round, are displayed in Figure 2b along with their docking scores. In general, the data set of 3225 compounds, which is only limited to the scaffolds of Figure 1b, shows in the docking simulations slightly lower docking scores and selectivity to the target site as compared to the top-ranking ligands found in the first round.

2.3. Measurements of inhibitory activity

Inhibitory activity was measured using a test of the 2′OMTase activity of NS5MTase$_{DV}$ that detects methylation of substrate ^{7Me}GpppAC$_5$ resulting in ^{7Me}GpppA$_{2'}$OMeC$_5$.[19] The bioassays showed low but measurable inhibition (between 5% and 45%) by all chosen compounds at a concentration of 100 μM except **7**, which rendered 75% inhibition (Fig. 4a). The bioassays of six compounds, **10**–**15**, from the second round of virtual screening did not identify better inhibitors (Fig. 4b). The results were obtained by applying a protocol where

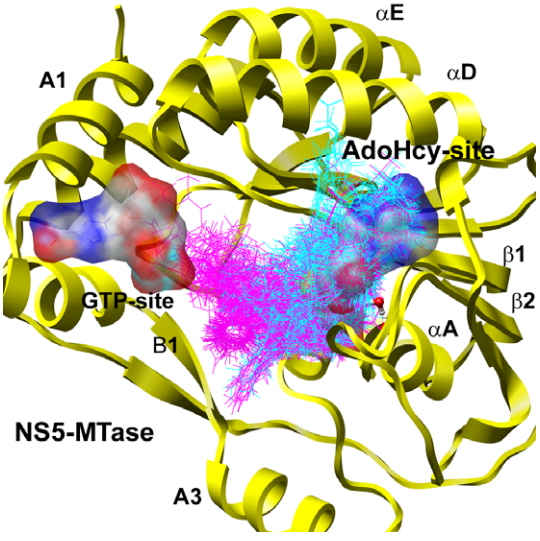

Figure 3. Overlayed docked positions of 230 ligands for the local (cyan) and global (magenta) docking simulations of the first round. Positions of the GTP- and AdoHcy-binding sites in NS5MTase$_{Dv}$ are delineated by the van der Waals surfaces of these compounds.

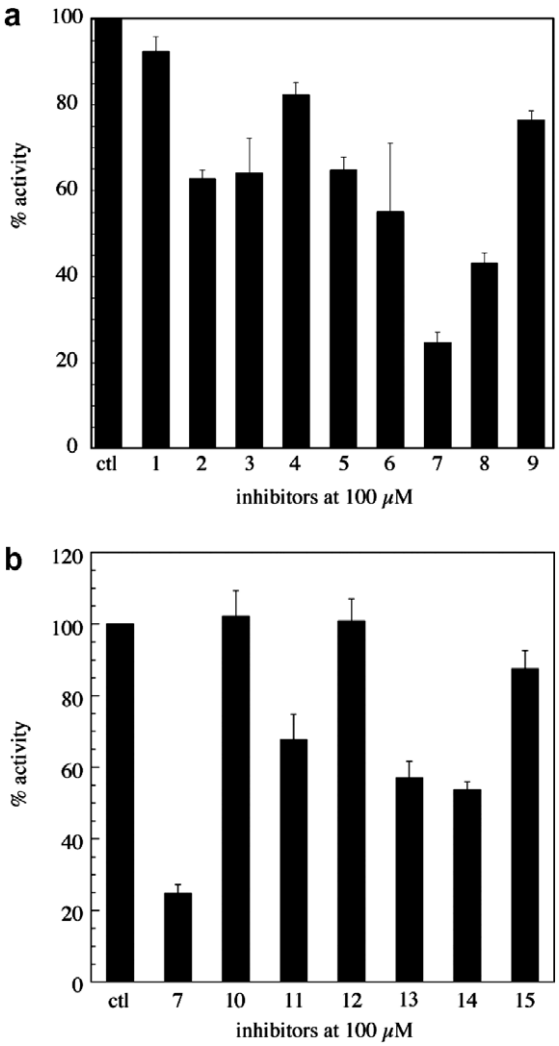

Figure 4. Biochemical tests of NS5MTase$_{Dv}$ inhibitor candidates. Inhibition of methylation of ^{7Me}GpppAC$_5$ substrates by NS5MTase$_{Dv}$ using 100 μM of each inhibitor candidate. Tests were conducted as described in Section 4.3. Ctl refers to the control test with 5% DMSO and no inhibitor. (a) Results from the first round. (b) Results from the second round. Compound **7** was included for comparison.

the reactions were started by adding the RNA substrate and cofactor AdoMet to a premix of enzyme and inhibitor. When an alternate protocol was used where the compounds were added to a premix of enzyme and RNA substrate and the reactions were then started by adding AdoMet, measured inhibition levels for weak inhibitors were generally lower and dramatically so for compound **7** (not shown). This observation suggests that the binding modes of these molecules, which are generally larger than AdoMet, also require part of the RNA substrate binding site for activity. The IC_{50} of compound **7** was determined using the first protocol (Fig. 5). An IC_{50} of 60.5 μM (±3.2 μM) was determined, which corresponds well to the obtained value of 25% activity at 100 μM showed in Figure 4a. Thus, compound **7** can be considered a moderately strong inhibitor of $NS5MTase_{DV}$, which competes with the cofactor AdoMet and presumably also the capped RNA substrate.

2.4. Analysis of the $NS5MTase_{DV}$-7 complex

It is of interest to compare the docked position of the newly determined inhibitor **7** with the pose of the bound AdoHcy in 1L9K (Fig. 6). The *p*-tolyl group of **7** in the docked complex is accommodated in the hydrophobic binding pocket for the adenine of AdoHcy. The hydrocarbon core of **7**, including the adamantane moiety, closely overlaps with AdoHcy in the region of the ribose ring. The carboxyl groups of AdoHcy and **7** also adopt similar positions at the polar part of the binding pocket. Both the (*R*) and (*S*) stereoisomers of **7** were among the top-docked solutions. In the bioassay studies compound **7** was tested as a racemic mixture. For global docking we considered the (*S*) stereoisomer (as in Fig. 6), which received slightly higher docking scores. Although it is not entirely straightforward to single out specific amino acids which determine the binding of **7**, without X-ray studies or more detailed free energy calculations, some interesting observations can be made. That is, several

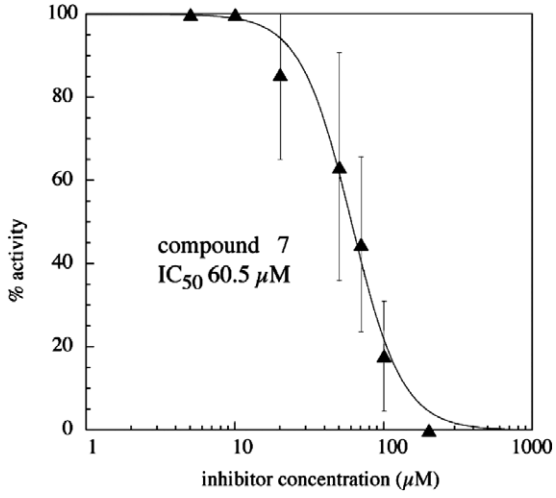

Figure 5. Determination of the IC_{50} value for compound **7**. The tested concentration range was 5–200 μM. Values were fitted to a dose–response curve as detailed in Section 4.3.

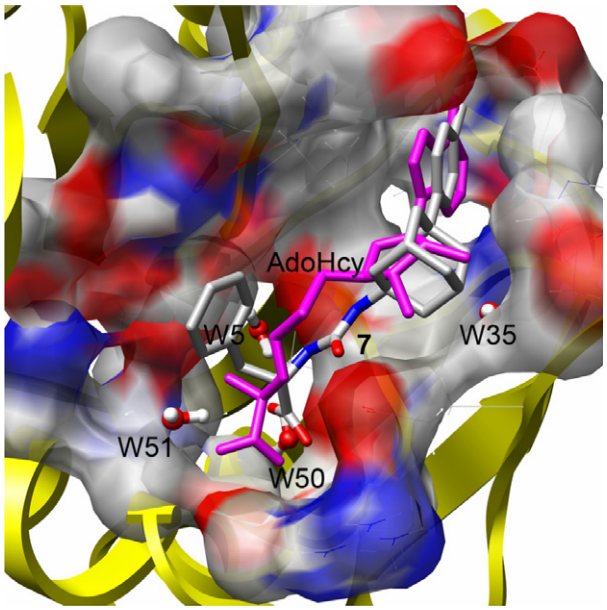

Figure 6. The experimental positions of AdoHcy (pink) and crystallographic waters, together with the docked pose of compound **7** in the $NS5MTase_{Dv}$ binding cleft.

of the potentially important polar interactions of AdoHcy in the binding site, that is, the adenine amino group with D131, the ribose ring with HOH35, G106, and E111 and the amino acid tail with HOH5, D79, and W87 (Fig. 1 of the Supplementary material), are apparently lost for **7** that has many nonpolar groups in its structure (Fig. 2 of the Supplementary material). Overall, the efficient binding of **7** appears to originate from a good complementary fit to the target site.

3. Conclusions

The virtual screening results suggested several new and previously unknown putative binders for the AdoMet-site in the $NS5MTase_{Dv}$ enzyme. The subsequent bioassay testing of their inhibitory effect on the 2′OMTase activity of $NS5MTase_{DV}$ demonstrated weak inhibitory effects for most considered structures, with compound **7** being the best inhibitor with an IC_{50} value of 60 μM. The new inhibitor **7** found in our work also shows pronounced docking selectivity for the AdoMet-binding site and consistently high scores both in the local and global docking runs. The predicted selective binding of **7** from the simulations can largely be attributed to the complementary fit with the target site. Identification of the active ligand **7** from a data set of 2.1 million compounds is an illustrative example of the general ability of virtual screening techniques to grasp essential features of ligand–protein interactions. In a second round of screening, we also searched for analogues of **7** among commercially available compounds. Note, in this respect, that the presence in the available database of active analogues for an active compound cannot be warranted in general at all. Indeed, the second round of virtual screening produced several compounds originating from the 2D substructure search based on **7**,

including the close analogue **14**, but only with lower inhibitory activity.

The identified inhibitor **7** may be a starting point for structure–activity studies where improvement of binding and inhibitory activity may be achieved via the synthesis of new molecules based on this scaffold. Such improved inhibitors could efficiently affect viral replication by binding to the AdoMet-binding site and thus inhibiting the N7- and 2′OMTase of $NS5MTase_{DV}$. Mutation of residue D146 situated very near the AdoMet-binding site and vital for both activities has been shown to be detrimental for replication of West Nile virus.[21] Cells transfected with an RNA containing the D146A mutation did not render any virus until days 3–4 post transfection.[20] Thus, a compound that binds to the AdoMet-binding site can therefore be expected to inhibit both activities and might be an efficient inhibitor of viral replication.

4. Experimental

4.1. Chemical database for virtual screening

The similarity and pharmacophore searches were performed using the Unity Chemical Information Software v.4.4.1 from Tripos Inc. (1699 South Hanley Road, St. Louis, Missouri, 63144, USA). The ligand states were prepared using the Ligprep program from Schrödinger LLC (120 West 45th Street, 32nd floor, New York, NY 10036-4041, USA).

The database of 2.1 million commercially available compounds included depositions from the following companies: Asinex Ltd., 5 Gabrichevskogo, St. Building 8, Moscow 125367, Russia; ChemBridge Corporation, 16981 Via Tazon, Suite G, San Diego, CA 92127, USA; ChemDiv, Inc., 11558 Sorrento Valley Road, San Diego, CA 92121, USA; Enamine Ltd., 23 Alexandra Matrosova Street, 01103 Kiev, Ukraine; InterBioScreen Ltd., PO Box 218, 119019 Moscow, Russia; Key Organics Ltd., Highfield Industrial Estate, Camelford, Cornwall PL32 9QZ, UK; Life Chemicals Inc., 2477 Glenwood School Drive Suite 203, Burlington, ON, L7R 3R9, Canada; Maybridge, Trevillet, Tintagel, Cornwall PL34 OHW, UK; Sigma–Aldrich, 3050 Spruce Street, St. Louis, MO 63103, USA; Specs, Kluyverweg 6, 2629 HT, Delft, The Netherlands; Vitas-M Laboratory Ltd., Center of Molecular Medicine, Vorobévi Gori, Moscow 119829, Russia.

4.2. Docking calculations

Docking computer simulations were performed using GOLD v.3.0[28,29] running under Linux. The program employs efficient scoring functions for describing molecular interactions, and a genetic algorithm (GA) for the minimization procedure. An all-atom model is used for the protein, crystallographic waters, and docked ligands. During sampling of the conformational space the ligands can adopt flexible conformations, some limited flexibility is allowed also for the protein side chains forming H-bonds with the ligand. The program also allows variable occupancies for crystallographic water sites[29] that apparently is of importance for the cases studied herein. The three-dimensional structure of the $NS5MTase_{Dv}$ target was taken from the PDB entry 1L9K.[15] Addition of hydrogens to the protein was done using DS ViewerPro 5.0 from Accelrys (www.accelrys.com). The ligand–protein interactions in the docked complexes were graphically mapped using Ligplot.[31] In order to reduce the computer time, the docking procedure was split into two steps. In the beginning, crude filtering of the large ligand sets was done using GA settings of 30,000 iterations for faster optimization. In the second step, the smaller sets of the top-ranking solutions were docked with GA settings for a sufficiently accurate search (200,000 iterations). Other GA settings in both steps were used according to the default values. The best solutions were selected from 10 GA runs for each ligand. The initial ligand sets were split into structural clusters that were docked separately in order to retain chemical diversity and not to lose interesting structures during crude docking.

4.3. Bioassay studies

4.3.1. Reagents. AdoMet was purchased from New England BioLabs. The tested compounds were purchased from InterBioScreen (**1**–**3**, **6** and **9**), Maybridge (**4**), Sigma–Aldrich (**5**), Life Chemicals (**7** and **14**), ChemDiv. (**8** and **10**), Vitas-M Laboratory (**11**), and Enamine (**12**, **13** and **15**). With regard to the stereoisomer composition the tested molecules are non-chiral or racemic mixtures, except for compounds **1**–**3** and **6**, where the amino acid building blocks correspond to either L- or D-amino acids. For **1**–**3**, L-Ile was used in the synthesis and for **6**, D-Val and L-Phe were used. Compounds were dissolved in DMSO and stored as 10 mM stock solutions at −20 °C.

The inhibitory activity of several predicted binders was tested on small RNA substrates $^{7Me}GpppAC_5$. All compounds were used at 100 μM final concentration. The MTase activity assays were performed in 30 μl samples containing 40 mM Tris, pH 7.5, 5 mM DTT, 5 μM AdoMet (0.3–2 μCi [^{3}H]AdoMet, Amersham Biosciences), 1 μM $NS5MTase_{DV}$, and 2 μM of RNA substrate $^{7Me}GpppAC_5$. Recombinant $NS5MTase_{DV}$ was produced as previously described.[15] Preparation of $^{7Me}GpppAC_5$ is described in Ref. 19 Two protocols to test inhibitor candidates were applied. In protocol A, inhibitor candidate solutions were added to a premix containing buffer and enzyme and the reactions were then started with a premix of AdoMet and RNA substrate. In protocol B reactions, inhibitor candidates were added to a pre-mix of enzyme and RNA substrate and reactions started with AdoMet. Inhibitor candidates were dissolved at 10 mM in DMSO. The operative concentrations are provided in the legend for Figure 4. Final concentration of DMSO in reaction mixtures was 1–5%, thus control reactions without inhibitor contain corresponding DMSO concentrations. Reactions were incubated at 30 °C. After 5 min, 14 μl samples were drawn and spotted into a well of 96-well sample plates contain-

ing 100 μl of 20 μM AdoHcy per well to stop the reaction. The background was measured by spotting 14 μl before the reaction started. The samples were then transferred to glass-fibre filtermats (DEAE filtermat, Wallac) by a Filtermat Harvester (Packard Instruments). Filtermats were washed twice with 0.01 M ammonium formate, pH 8.0, twice with water and once with ethanol, dried and transferred into sample bags. Liquid scintillation fluid was added and methylation of RNA substrates was measured in counts per minute (cpm) by using a Wallac MicroBeta TriLux Liquid Scintillation Counter. The IC_{50} (inhibitor concentration at 50% activity) value of compound **7** was determined using protocol A. Two independent experiments were done. Data were adjusted to a logistic dose–response function (% activity = $100/(1 + [I]/IC_{50})^b$, where b corresponds to the slope factor that determines the slope of the curve[32]).

Acknowledgment

Support from the EU VIZIER program (CT 2004-511960) is gratefully acknowledged.

Supplementary data

Supplementary data associated with this article can be found, in the online version, at doi:10.1016/j.bmc.2007.08.049.

References and notes

1. De Clercq, E. *Nat. Rev. Microbiol.* **2004**, *2*, 704.
2. Bisaillon, M.; Lemay, G. *Virology* **1997**, *236*, 1.
3. Furuichi, Y.; Shatkin, A. J. *Adv. Virus Res.* **2000**, *55*, 135.
4. Voet, D.; Voet, J. G. *Biochemistry*, third ed.; Wiley & Sons, Inc: New York, 2004, pp. 1254–1255.
5. Borchardt, R. T. *J. Med. Chem.* **1980**, *23*, 347.
6. Benkovic, S. J.; Baker, S. J.; Alley, M. R. K.; Woo, Y.-H.; Zhang, Y.-K.; Akama, T.; Mao, W.; Baboval, J.; Rajagopalan, P. T. R.; Wall, M.; Kahng, L. S.; Tavassoli, A.; Shapiro, L. *J. Med. Chem.* **2005**, *48*, 7468.
7. Mashhoon, N.; Pruss, C.; Carroll, M.; Johnson, P. H.; Reich, N. O. *J. Biomol. Screen.* **2006**, *11*, 497.
8. Kreander, K.; Kurkela, M.; Siiskonen, A.; Vuorela, P.; Tammela, P. *Pharmazie* **2006**, *61*, 247.
9. Woyciniuk, P.; Linder, M.; Scholtissek, C. *Virus Res.* **1995**, *35*, 91.
10. Hanessian, S.; Sgarbi, P. W. M. *Bioorg. Med. Chem. Lett.* **2000**, *10*, 433.
11. Chrebet, G. L.; Wisnievski, D.; Perkins, A. L.; Deng, Q.; Kurtz, M. B.; Marcy, A.; Parent, S. A. *J. Biomol. Screening* **2005**, *10*, 355.
12. Schwer, B.; Lehmans, K.; Saha, N.; Shuman, S. *J. Biol. Chem.* **2001**, *276*, 1857.
13. Taylor, S. M.; Jones, P. A. *J. Mol. Biol.* **1982**, *162*, 679.
14. Fiala, E. S.; Staretz, M. E.; Pandya, G. A.; El-bayoumy, K.; Hamilton, S. R. *Carcinogenesis* **1998**, *19*, 597.
15. Egloff, M.-P.; Benarroch, D.; Selisko, B.; Romette, J.-L.; Canard, B. *EMBO J.* **2002**, *21*, 2757.
16. Benarroch, D.; Egloff, M.-P.; Mulard, L.; Guerreiro, C.; Romette, J.-L.; Canard, B. *J. Biol. Chem.* **2004**, *279*, 35638.
17. Fauman, E. B.; Blumenthal, R. M.; Cheng, X. Structure and evolution of AdoMet-dependent methyltransferases. In *S-Adenosylmethionine-Dependent Methyl-transferases: Structure and Functions*; Chen, X., Blumenthal, R. M., Eds.; World Scientific Publishing: Singapore, 1999; pp 1–38.
18. Martin, J. L.; McMillan, F. M. *Curr. Opin. Struct. Biol.* **2002**, *12*, 783.
19. Peyrane, F.; Selisko, B.; Decroly, E.; Vasseur, J. J.; Benarroch, D.; Canard, B.; Alvarez, K. *Nucleic Acid Res.* **2007**, *35*, e26.
20. Zhou, Y.; Ray, D.; Zhao, Y.; Dong, H.; Ren, S.; Li, Z.; Guo, Y.; Bernard, K. A.; Shi, P.-Y.; Li, H. *J. Virol.* **2007**, *81*, 3891.
21. Ray, D.; Shah, A.; Tilgner, M.; Guo, Y.; Zhao, Y.; Dong, H.; Deas, T. S.; Zhou, Y.; Li, H.; Shi, P.-Y. *J. Virol.* **2006**, *80*, 8362.
22. Abagyan, R.; Totrov, M. *Curr. Opin. Chem. Biol.* **2001**, *5*, 375.
23. Doman, T. N.; McGovern, S. L.; Witherbee, B. J.; Kasten, T. P.; Kurumbail, R.; Stallings, W. C.; Connolly, D. T.; Shoichet, B. K. *J. Med. Chem.* **2002**, *45*, 2213.
24. Rastelli, G.; Pacchioni, S.; Sirawaraporn, W.; Sirawaraporn, R.; Parenti, M. D.; Ferrari, A. M. *J. Med. Chem.* **2003**, *46*, 2834.
25. Kitchen, D. B.; Decornez, H.; Furr, J. R.; Bajorath, J. *Nat. Rev. Drug Discov.* **2004**, *3*, 935.
26. Congreve, M.; Murray, C. W.; Blundell, T. L. *Drug Discovery Today* **2005**, *10*, 895.
27. Alonso, H.; Bliznyuk, A. A.; Gready, J. E. *Med. Res. Rev.* **2006**, *26*, 531.
28. Jones, G.; Willet, P.; Glen, R. C.; Leach, A. R.; Taylor, R. *J. Mol. Biol.* **1997**, *267*, 727.
29. Verdonk, M.; Chessari, G.; Cole, J. C.; Hartshorn, M. J.; Murray, C. W.; Nissink, J. W.; Taylor, R. D.; Taylor, R. *J. Med. Chem.* **2005**, *48*, 6504.
30. Baxter, C. A.; Murray, C. W.; Clark, D. E.; Westhead, D. R.; Eldridge, M. D. *Proteins* **1998**, *33*, 367.
31. Wallace, A. C.; Laskowski, R. A.; Thornton, J. M. *Protein Eng.* **1995**, *8*, 127.
32. DeLean, A.; Munson, P. J.; Rodbard, D. *Am. J. Physiol.* **1978**, *235*, E97.